Structural Effects in the Indanedione Skeleton for the Design of Low Intensity 300–500 nm Light Sensitive Initiators

ARTICLE *in* MACROMOLECULES · DECEMBER 2013

Impact Factor: 5.8 · DOI: 10.1021/ma402149g

CITATIONS
17

READS
25

8 AUTHORS, INCLUDING:

Pu Xiao
Université de Haute-Alsace
77 PUBLICATIONS **630** CITATIONS
SEE PROFILE

Frédéric Dumur
Aix-Marseille Université
158 PUBLICATIONS **1,875** CITATIONS
SEE PROFILE

Fabrice Morlet-Savary
Université de Haute-Alsace
171 PUBLICATIONS **2,322** CITATIONS
SEE PROFILE

Jacques Lalevée
Université de Haute-Alsace
338 PUBLICATIONS **4,057** CITATIONS
SEE PROFILE

Macromolecules

Article

pubs.acs.org/Macromolecules

Structural Effects in the Indanedione Skeleton for the Design of Low Intensity 300−500 nm Light Sensitive Initiators.

Pu Xiao,[†] Frédéric Dumur,[‡,§,∥] Bernadette Graff,[†] Fabrice Morlet-Savary,[†] Loïc Vidal,[†] Didier Gigmes,*[,‡] Jean Pierre Fouassier,[⊥] and Jacques Lalevée*[,†]

[†]Institut de Science des Matériaux de Mulhouse IS2M, UMR CNRS 7361, UHA, 15 rue Jean Starcky, 68057 Mulhouse Cedex, France

[‡]Institut de Chimie Radicalaire, Aix-Marseille Université, CNRS, Institut de Chimie Radicalaire ICR, UMR 7273, F-13397 Marseille, France

[§]Université Bordeaux, IMS, UMR 5218, F-33400 Talence, France

[∥]CNRS, IMS, UMR 5218, F-33400 Talence, France

Supporting Information

ABSTRACT: Newly synthesized indanedione derivatives combined with an iodonium salt, *N*-vinylcarbazole, amine, phenacyl bromide, or 2,4,6-tris-(trichloromethyl)-1,3,5-triazine have been used as photoinitiating systems upon very low visible light intensities: blue lights (e.g., household blue LED bulb at 462 nm) or even a halogen lamp exposure. One of them (ID2) is particularly efficient for cationic, radical and thiol−ene photopolymerizations as well as for the synthesis of interpenetrated polymer networks (IPNs). It can be useful to overcome the oxygen inhibition. ID2 based photoinitiating systems can also be selected for the reduction of Ag^+ and the in situ formation of Ag(0) nanoparticles in the synthesized polymers. The (photo)chemical mechanisms are studied by electron spin resonance spin trapping, fluorescence, cyclic voltammetry, laser flash photolysis, and steady state photolysis techniques.

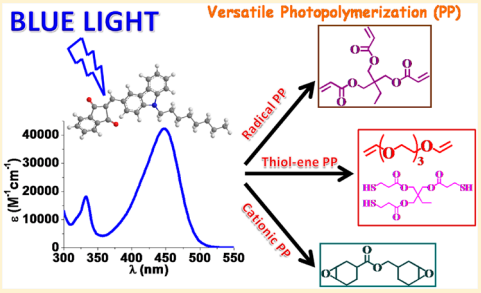

INTRODUCTION

Dye is one of the most important components in monomer/oligomer formulations photopolymerizable under visible lights as it can lead, through interactions with suitable additives to initiating radicals (for free radical polymerization (FRP) or thiol−ene polymerization), cations or radical cations (for cationic polymerization (CP) or free radical promoted cationic polymerization (FRPCP)). It is of great interest to develop novel high performance dyes for visible light sensitive polymerization reactions for applications in radiation curing, medicine, microelectronics, nanotechnology, imaging and optics technologies, or material elaboration areas.[1−4] The introduction of suitable substituents into known UV light sensitive compounds or colored structures as well as the design of novel skeletons allows a red-shifted light absorption; sometimes, it also significantly increases the molar extinction coefficients ε. Recent examples of initiating systems can be seen in refs 1 and 5−7, but relatively high light intensities are used for the polymerization.

In a recent study,[8] two indanedione derivatives ID (containing an aniline or a pyrene moiety—noted D_1 and D_2 in Scheme 1, respectively) have been developed as push−pull photoinitiators. They are based on a D-π-A structure (D is the electron donor moiety of the molecule and A the electron acceptor) that allowed a blue-to-red light sensitivity and an efficient polymerization ability for D_1. On the opposite, D_2 was inefficient, which shows a strong structure/reactivity relationship for this new class of ID dyes.

For a better understanding of the ID photochemical/chemical reactivity, four new derivatives (an indanedione moiety linked to an alkyl phenyl moiety (ID1), a carbazole moiety (ID2), an anthracene moiety (ID3), or two indanedione moieties linked to each other though a phenyl ring (ID4)) have been designed and prepared (Scheme 1). The substituents are expected to have different and probably better effects on the light absorption properties, the involved chemical mechanisms and subsequently the photoinitiating abilities for the CP of epoxide and divinyl ether monomers, the FRP of acrylates, the hybrid cure of acrylate/epoxide blends and the thiol-divinylether photopolymerization under very soft irradiation conditions (~10 mW cm^{-2}) using a halogen lamp or a household blue LED (a 100 mW cm^{-2} blue laser diode will also be employed to check intensity effects). The ID2-based photoinitiating systems can also be used for UV LED irradiations (e.g., 365, 385, or 395 nm). Remarkably, these photoinitiating systems can also be used for the in situ formation of Ag(0) nanoparticles in the synthesized polymers through the reduction of a silver salt. The photochemical mechanisms involved in the initiation species formation will be

Received: October 18, 2013
Revised: November 6, 2013
Published: December 27, 2013

Scheme 1. Chemical Structures of the New Studied Indanedione Derivatives (ID1−ID4) and Previously Investigated Compounds D_1 and D_2

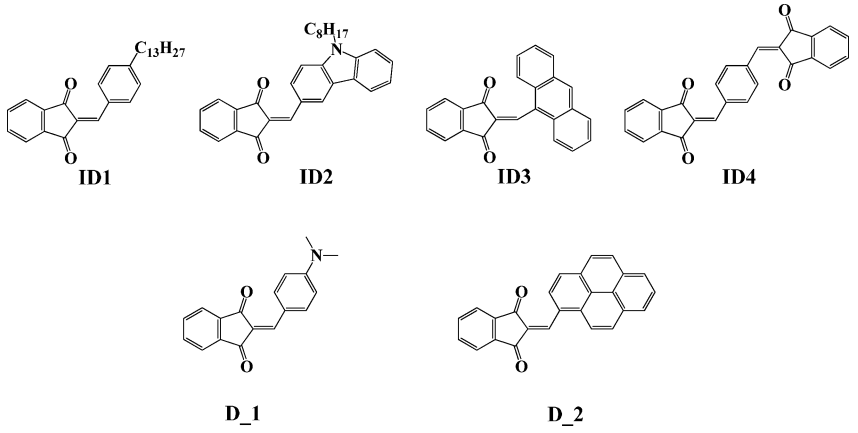

Scheme 2. Chemical Structures of Additives and Monomers

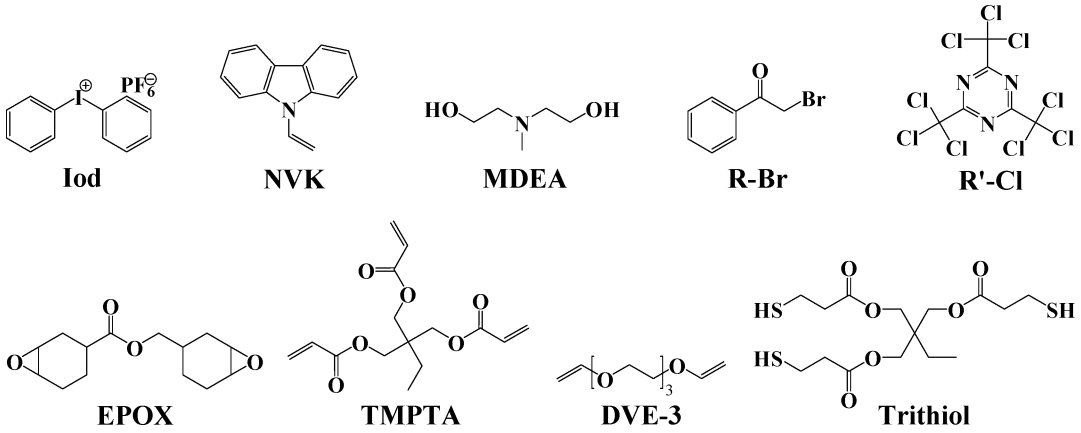

investigated by electron spin resonance spin trapping, fluorescence, cyclic voltammetry, laser flash photolysis, and steady state photolysis techniques.

EXPERIMENTAL SECTION

Materials. The investigated indanedione derivatives ID*n* (i.e., ID1−ID4) and other chemical compounds are shown in Schemes 1 and 2. Diphenyliodonium hexafluorophosphate (Iod), *N*-vinylcarbazole (NVK), methyl diethanolamine (MDEA), phenacyl bromide (R−Br), 2,4,6-tris(trichloromethyl)-1,3,5-triazine (R′−Cl), tri(ethylene glycol) divinyl ether (DVE-3), trimethylolpropane tris(3-mercaptopropionate) (Trithiol), and the other reagents and solvents were purchased from Sigma-Aldrich or Alfa Aesar with the highest purity available and used as received. The monomers (3,4-epoxycyclohexane)methyl 3,4-epoxycyclohexylcarboxylate (EPOX) and trimethylolpropane triacrylate (TMPTA) were obtained from Cytec and used as benchmark monomers for cationic and radical photopolymerizations.

Synthesis of the Indanedione Derivatives. Mass spectroscopy was performed by the Spectropole of Aix-Marseille University. ESI mass spectral analyses were recorded with a 3200 QTRAP (Applied Biosystems SCIEX) mass spectrometer. The HRMS mass spectral analysis was performed with a QStar Elite (Applied Biosystems SCIEX) mass spectrometer. Elemental analyses were recorded with a Thermo Finnigan EA 1112 elemental analysis apparatus driven by the Eager 300 software. ^{1}H and ^{13}C NMR spectra were determined at room temperature in 5 mm o.d. tubes on a Bruker Avance 400 spectrometer of the Spectropole: ^{1}H (400 MHz) and ^{13}C (100 MHz). The ^{1}H chemical shifts were referenced to the solvent peak $CDCl_3$ (7.26 ppm), DMSO (2.49 ppm) and the ^{13}C chemical shifts were referenced to the solvent peak $CDCl_3$ (77 ppm), DMSO (49.5 ppm). All these indanedione derivatives were prepared with analytical purity up to accepted standards for new organic compounds (>98%) which was checked by high field NMR analysis.

*Synthesis of 2-(4-Tridecylbenzylidene)-1H-indene-1,3(2H)-dione (**ID1**).* Methyl 4-tridecylbenzoate,[9] (4-tridecylphenyl)methanol, and (4-tridecylphenyl)methanal[10] used for the synthesis of **ID1** were prepared as previously reported. 4-Tridecylbenzaldehyde (3.94 g, 13.66 mmol) and indane-1,3-dione (2 g, 13.66 mmol) were dissolved in absolute ethanol (100 mL). A few drops of piperidine were added. Immediately, the solution turned purple. The solution was refluxed for 4 h. After cooling, the precipitate was filtered off, washed several times with ether, and dried under vacuum (5.35 g, 94% yield). ^{1}H NMR ($CDCl_3$), δ (ppm): 0.88 (t, 3H, J = 6.6 Hz), 1.26−1.32 (m, 20H), 1.65 (qt, 2H, J = 7.0 Hz), 2.69 (t, 2H, J = 7.6 Hz), 7.33 (d, 2H, J = 8.2 Hz), 7.80−7.82 (m, 2H), 7.89 (s, 1H), 7.99−8.02 (m, 2H), 8.42 (d, 2H, J = 8.2 Hz). ^{13}C NMR ($CDCl_3$), δ (ppm): 14.1, 22.7, 29.31, 29.35, 29.47, 29.55, 29.64, 29.67, 31.0, 31.9, 36.3, 123.22, 123.25, 128.2, 129.0, 130.8, 134.5, 135.0, 135.2, 140.1, 142.5, 147.2, 149.7, 189.2, 190.5; HRMS (ESI MS) m/z: theor, 417.2788; found, 417.2790 ($[M + H]^+$ detected).

*Synthesis of 2-((9-Octyl-9H-carbazol-3-yl)methylene)-1H-indene-1,3(2H)-dione (**ID2**).* 9-Octyl-9*H*-carbazole-3-carbaldehyde used for the synthesis of **ID2** was synthesized as reported without modification and in similar yield.[11]

9-Octyl-9*H*-carbazole-3-carbaldehyde (4.21 g, 13.69 mmol) and indane-1,3-dione (2 g, 13.69 mmol) were dissolved in absolute ethanol (200 mL). A few drops of piperidine were added. Immediately, the solution turned purple. The solution was refluxed for 4 h. After cooling, the precipitate was filtered off, washed several times with ether and dried under vacuum. A few conversion of the aldehyde was

dx.doi.org/10.1021/ma402149g | *Macromolecules* 2014, 47, 26−34

detected. Indane-1,3-dione (2 g, 13.69 mmol) was added to the former precipitate; 100 mL absolute ethanol was added followed by a few drops of piperidine. The solution was refluxed overnight. The solvent was removed under reduced pressure. The residue was purified by column chromatography (SiO_2) using DCM:pentane 1:1 as the eluent. The product was eluted as the first fraction. After evaporation of the volatiles, dissolution in ether followed by addition of pentane precipitated a light yellow solid which was filtered off, washed several times with pentane and dried under vacuum (5.12 g, 86% yield). ^{1}H NMR ($CDCl_3$), δ (ppm): 0.85 (t, 3H, J = 6.8 Hz), 1.23−1.33 (m, 10H), 1.86 (qt, 2H, J = 6.7 Hz), 4.26 (t, 2H, J = 7.1 Hz), 7.28−7.50 (m, 4H), 7.72−7.75 (m, 2H), 7.93−7.97 (m, 2H), 8.03 (s, 1H), 8.21 (d, 1H, J = 7.7 Hz), 8.62 (d, 1H, J = 8.6 Hz), 9.39 (s, 1H). ^{13}C NMR ($CDCl_3$), δ (ppm): 14.1, 22.6, 27.3, 28.9, 29.1, 29.3, 31.8, 43.4, 108.9, 109.4, 120.5, 121.0, 122.8, 123.2, 123.6, 124.9, 125.4, 126.6, 128.7, 133.3, 134.5, 134.8, 139.9, 141.0, 142.4, 143.7, 148.7, 189.7, 191.1. HRMS (ESI MS) m/z: theor, 435.2198; found, 435.2199 ($M^{+\bullet}$ detected).

*Synthesis of 2-(Anthracen-9-ylmethylene)-1H-indene-1,3(2H)-dione (**ID3**).* 9-Anthracenealdehyde (2.82 g, 13.67 mmol) and indane-1,3-dione (2 g, 13.67 mmol) were dissolved in absolute ethanol (100 mL). A few drops of piperidine were added, and the reaction mixture was refluxed for 3 h. The solvent was removed under reduced pressure. The residue was purified by column chromatography (SiO_2) using DCM as the eluent. The product was eluted as the first band (3.74 g, 82% yield). ^{1}H NMR ($CDCl_3$), δ (ppm): 7.48−7.53 (m, 4H), 7.81−7.85 (m, 3H), 7.97−8.00 (m, 2H), 8.05−8.08 (m, 2H), 8.12−8.15 (m, 1H), 8.58 (s, 1H), 8.91 (s, 1H). ^{13}C NMR ($CDCl_3$), δ (ppm): 123.5, 123.6, 125.4, 125.5, 126.8, 129.1, 129.9, 130.4, 131.0, 134.0, 135.4, 135.6, 140.8, 141.7, 142.7, 187.5, 189.3. HRMS (ESI MS) m/z: theor, 334.0994; found, 334.0997 ($M^{+\bullet}$ detected).

*Synthesis of 2,2′-(1,4-Phenylenebis(methanylylidene))bis(1H-indene-1,3(2H)-dione) (**ID4**).* Terephthaldehyde (0.91 g, 6.78 mmol) and indane-1,3-dione (2 g, 13.56 mmol, 2 equiv) were dissolved in absolute ethanol (100 mL). A few drops of piperidine were added. Immediately, the solution turned bordeaux red. The solution was refluxed for 4 h. After cooling, the yellow precipitate was filtered off, washed several times with ether, and dried under vacuum (1.95 g, 74% yield). ^{1}H NMR (DMSO-d_6), δ (ppm): 7.95−8.06 (m, 8H), 8.63 (s, 4H). HRMS (ESI MS) m/z: theor, 390.0892; found, 390.0888 ($M^{+\bullet}$ detected). Anal. Calcd for $C_{26}H_{14}O_4$: C, 80.0; H, 3.6; O, 16.4. Found: C, 80.1; H, 3.4; O, 16.7.

Irradiation Sources. Different visible irradiation sources were used for the photopolymerization experiments: (i) polychromatic light from a halogen lamp (Fiber-Lite, DC-950; incident light intensity ∼ 12 mW cm^{-2} in the 370−800 nm range), (ii) laser diode at 457 nm (100 mW cm^{-2}), (iii) a low intensity 385 nm LED (ML385-L2 − ThorLabs; ∼9 mW cm^{-2}), and (iv) a household blue LED bulb centered at 462 nm (∼10 mW cm^{-2}).

Photopolymerization Experiments. For photopolymerization experiments, the conditions are given in the figure captions. The photosensitive formulations were deposited on a BaF_2 pellet under air or in laminate (25 μm thick) for irradiation with different lights. The evolution of the epoxy group content of EPOX, the double bond content of TMPTA, the double bond content of DVE-3 and the thiol (S−H) content of Trithiol were continuously followed by real time FTIR spectroscopy (JASCO FTIR 4100)[12,13] at about 790, 1630, 1620, and 2580 cm^{-1}, respectively. The conversions of NVK were not measured in TMPTA.

ESR Spin Trapping (ESR-ST) Experiments. ESR-ST experiments were carried out using a X-Band spectrometer (MS 400 Magnettech). The radicals were generated at room temperature upon visible light exposure (e.g., halogen lamp) under N_2 and trapped by phenyl-*N*-*tert*-butylnitrone (PBN) according to a procedure[14] described elsewhere in detail. The ESR spectra simulations were carried out with the WINSIM software.

Fluorescence Experiments. The fluorescence properties of the investigated IDs were studied in acetonitrile using a JASCO FP-750 spectrometer. The interaction IDs/Iod can be investigated through classical Stern−Volmer treatments.[15]

Redox Potentials. The oxidation potentials (E_{ox} vs SCE) of the IDs were measured in acetonitrile by cyclic voltammetry with tetrabutylammonium hexafluorophosphate (0.1 M) as a supporting electrolyte (Voltalab 6 Radiometer). The working electrode was a platinum disk and the reference electrode was a saturated calomel electrode (SCE). Ferrocene was used as a standard, and the potentials determined from the half peak potential were calibrated to the reversible formal potential of this compound (+0.44 V/SCE). The free energy change ΔG for an electron transfer between the studied IDs and Iod can be easily calculated from the classical Rehm−Weller equation (eq I, where E_{ox}, E_{red}, E_S (or E_T), and C are the oxidation potential of the studied indanedione derivatives, the reduction potential of Iod, the excited singlet (or triplet) state energy of the studied indanedione derivatives, and the electrostatic interaction energy for the initially formed ion pair, generally considered as negligible in polar solvents):[16]

$$\Delta G = E_{ox} - E_{red} - E_S \text{ (or } E_T) + C \quad \text{(I)}$$

Computational Procedure. Molecular orbital calculations were carried out with the Gaussian 03 suite of programs. The electronic absorption spectra for the different compounds were calculated with the time-dependent density functional theory at B3LYP/6-31G* level on the relaxed geometries calculated at UB3LYP/6-31G* level.[17,18]

Laser Flash Photolysis. Nanosecond laser flash photolysis (LFP) experiments were carried out using a Q-switched nanosecond Nd/YAG laser at λ_{exc} = 355 nm (9 ns pulses; energy reduced down to 10 mJ; minilite Continuum); the analyzing system (Luzchem LFP 212) consisted of a ceramic xenon lamp, a monochromator, a fast photomultiplier and a transient digitizer.[19]

Transmission Electron Microscopy (TEM). Observations were conducted on a Philips CM200 microscope operating at an acceleration voltage of 200 kV. For metal nanoparticles in acetonitrile, the suspension was deposited on a carbon coated copper grid. Once the acetonitrile was evaporated at room temperature, it left a distribution of particles on the support.

RESULTS AND DISCUSSION

1. Light Absorption Properties of the Studied Indanedione Derivatives. The absorption spectra of the investigated IDn (ID1-ID3) in acetonitrile are given in Figure 1. The difunctional derivative ID4 whose absorption maxima is

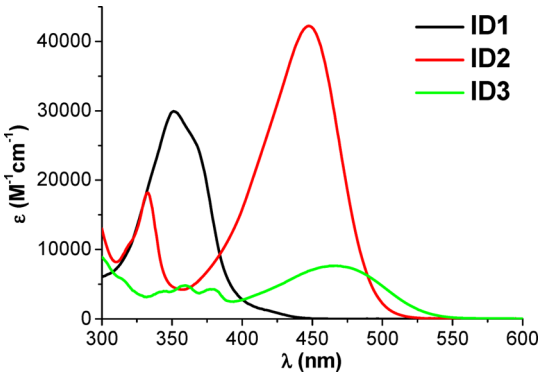

Figure 1. UV−vis absorption spectra of the studied indanedione derivatives in acetonitrile.

located at 389 nm (ε > 26900 M^{-1} cm^{-1}) has a poor solubility in organic solvents (e.g., acetonitrile, acetone, etc.) probably due to its bulky and symmetric chemical structure. The absorption of ID1 is mainly located in the UV range (λ_{max} = 351 nm, $\varepsilon_{351\ nm}$ = 29900 M^{-1} cm^{-1}) and exhibits a little overlapping with the emission spectra of the halogen lamp. Interestingly, ID2 and ID3 show a better absorption in the visible wavelength range (λ_{max} = 448 nm, $\varepsilon_{448\ nm}$ = 42200 M^{-1}

dx.doi.org/10.1021/ma402149g | Macromolecules 2014, 47, 26−34

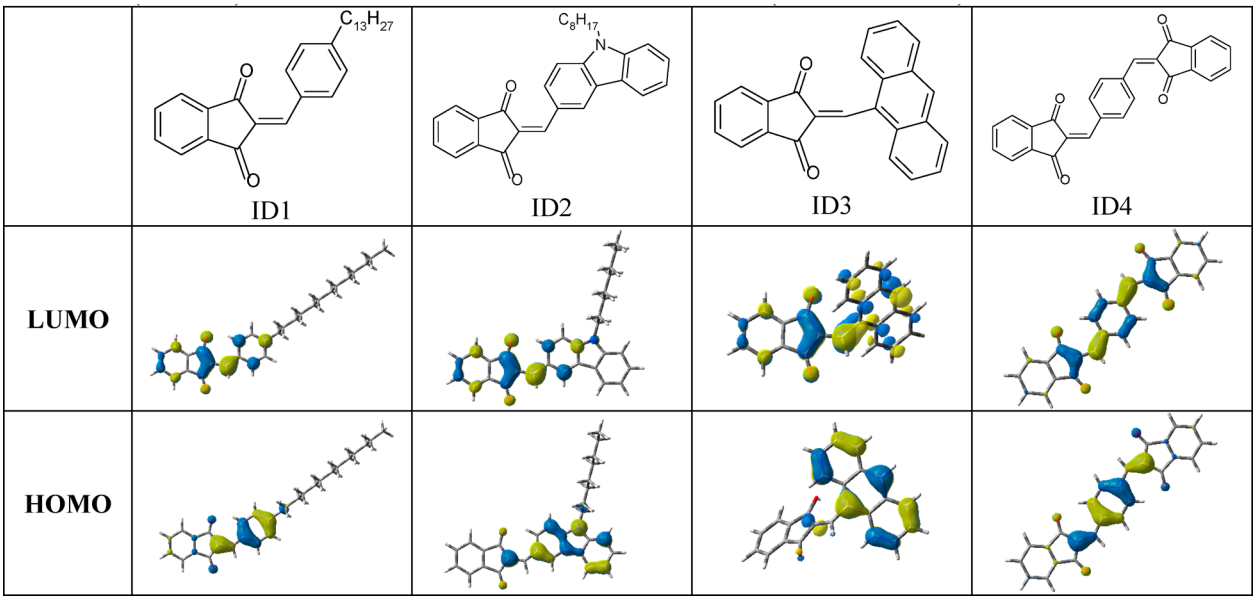

Figure 2. Highest occupied molecular orbitals (HOMO) and lowest unoccupied molecular orbitals (LUMO) for **ID1**–**ID4** at UB3LYP/6-31G* level (isovalue = 0.04).

cm^{-1} and λ_{max} = 467 nm, $\varepsilon_{467\ nm}$ = 7700 M^{-1} cm^{-1} for ID2 and ID3, respectively) than that of an indanedione, a carbazole or an anthracene moiety, which is due to the important charge transfer occurring in the electronic transition.[8] Compared to our previously studied D_1 derivative (λ_{max} = 478 nm, $\varepsilon_{478\ nm}$ = 38000 M^{-1} cm^{-1}),[8] the ε of ID2 is even higher (e.g.: $\varepsilon_{448\ nm}$ = 42200 M^{-1} cm^{-1}). The ID2 absorption spectrum allows an interesting matching with the emission spectra of the different light sources: the halogen lamp, the laser diodes at 457 nm ($\varepsilon_{457\ nm}$ = 38600 M^{-1} cm^{-1}) and 405 nm ($\varepsilon_{405\ nm}$ = 18 600 M^{-1} cm^{-1}), the household blue LED bulb centered at 462 nm ($\varepsilon_{462\ nm}$ = 33900 M^{-1} cm^{-1}) and UV LEDs at 385 nm ($\varepsilon_{385\ nm}$ = 9600 M^{-1} cm^{-1}) or 395 nm ($\varepsilon_{395\ nm}$ = 13 300 M^{-1} cm^{-1}). As to ID3, an acceptable matching is also observed but to a lesser extent (e.g.: $\varepsilon_{457\ nm}$ = 7500 M^{-1} cm^{-1}).

The highest occupied molecular orbitals (HOMO) are mainly located on the carbazole and anthracence moieties for ID2 and ID3, respectively; the lowest unoccupied molecular orbitals (LUMO) lie on the indanedione skeleton. Therefore, the excellent visible light absorption properties of ID2 and ID3 are associated with the high charge transfer character of the lowest energy transition; this $\pi \rightarrow \pi^*$ band is associated with the HOMO → LUMO transition (Figure 2).

2. Photoinitiating Ability of the Investigated Indanedione Derivatives. *2a. Cationic Photopolymerization of Epoxides.* Typical conversion–time profiles for the photopolymerization of EPOX in the presence of IDn/Iod or IDn/Iod/NVK PISs under air are displayed in Figure 3 (halogen lamp or 457 nm laser diode; conversions for 800 s of irradiation summarized in Table 1; Iod alone is not efficient as it works below 300 nm[15,20]). In the presence of ID1 (or ID3)/Iod or ID1 (or ID3)/Iod/NVK combinations, no polymerization of EPOX was observed (too low absorption, see Figure 1). The ID4/Iod does not work (halogen lamp irradiation), but the addition of NVK (as elsewhere in other systems[21]) significantly enhances the polymerization profile but the conversion remains low (33% at t = 800 s; Figure 3, curve 4). Interestingly, ID2/Iod and ID2/Iod/NVK exhibit a very good efficiency and lead to the formation of tack free coatings with conversion of 56%

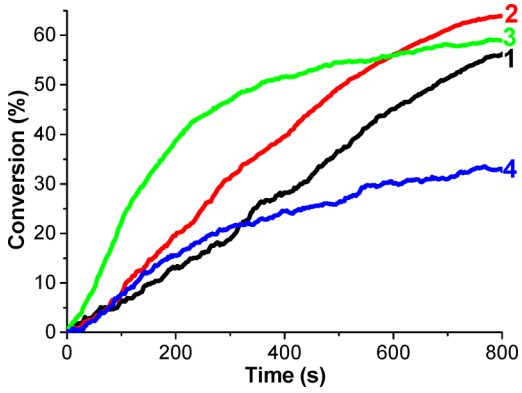

Figure 3. Photopolymerization profiles of EPOX under air in the presence of ID2/Iod (0.5%/2%, w/w) upon the halogen lamp (curve 1); ID2/Iod/NVK (0.5%/2%/3%, w/w/w) upon the halogen lamp (curve 2) and laser diode at 457 nm (curve 3) exposure; ID4/Iod/NVK (0.5%/2%/3%, w/w/w) upon the halogen lamp exposure (curve 4).

Table 1. EPOX Conversions Obtained under Air upon Exposure to Different Visible Light Sources for 800 s in the Presence of ID*n*/Iod (0.5%/2%, w/w) or ID*n*/Iod/NVK (0.5%/2%/3%, w/w/w)[a]

IDn	halogen lamp	laser diode 457 nm
ID1	np[b,c]	–
ID2	56%,[b] 64%[c]	59%[c]
ID3	np[b,c]	np[c]
ID4	np,[b] 33%[c]	–

[a]np: no polymerization. [b]IDn/Iod (0.5%/2%, w/w). [c]IDn/Iod/NVK (0.5%/2%/3%, w/w/w).

and 64% at t = 800 s (halogen lamp; Figure 3, curve 1 and curve 2). A higher polymerization rate with a little lower conversion (59%; Figure 3, curve 3 vs curve 2) is noted with ID2/Iod/NVK at 457 nm as resulting from the higher light intensity of the diode laser (100 mW cm^{-2}). The new ID2/Iod and ID2/Iod/NVK combinations are better than the previously

dx.doi.org/10.1021/ma402149g | *Macromolecules* 2014, 47, 26–34

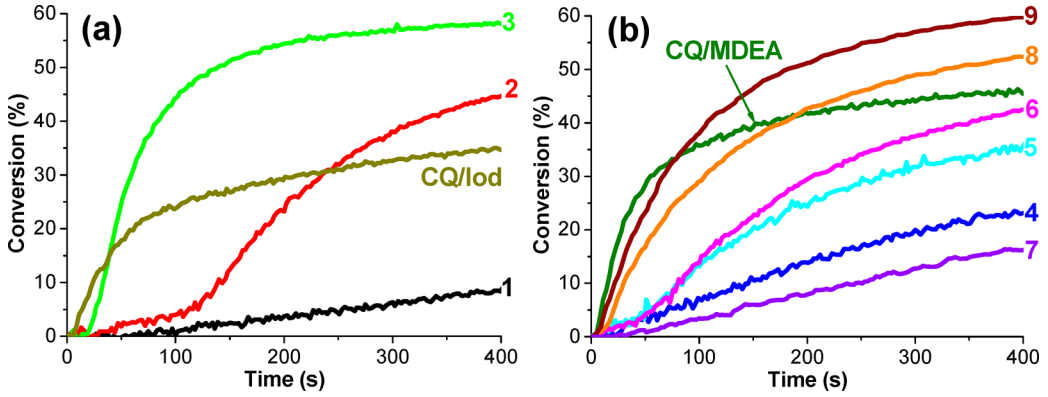

Figure 4. Photopolymerization profiles of TMPTA in laminate in the presence of (i) ID2/Iod (0.5%/2%, w/w) upon the halogen lamp (curve 1) or the laser diode at 457 nm (curve 2) exposure; ID2/Iod/NVK (0.5%/2%/3%, w/w/w) at 457 nm exposure (curve 3); (ii) ID2/MDEA (0.5%/2%, w/w) upon the halogen lamp (curve 4) or at 457 nm (curve 5); ID2/MDEA/R−Br (0.5%/2%/3%, w/w/w) at 457 nm (curve 6); (iii) ID2/R′−Cl (0.5%/1%, w/w) (curve 7); ID2/MDEA/R′−Cl(1) (0.5%/2%/1%, w/w/w) (curve 8); ID2/MDEA/R′−Cl(3) (0.5%/2%/3%, w/w/w) (curve 9) at 457 nm; (iv) CQ/Iod (0.5%/2%, w/w) or CQ/MDEA (0.5%/2%, w/w) as references at 457 nm.

reported D_1/Iod or D_1/Iod/NVK systems (halogen lamp; conversion <35% at t = 800 s).[8] Remarkably, in the same conditions, the known CQ (camphorquinone)/Iod[1] or even CQ/Iod/NVK systems are not efficient. ID2/Iod/NVK can also be used for UV LED exposure at 385 nm leading to tack free coatings (61% of conversion for 1000s of irradiation); this can be ascribed to the excellent light absorption properties of ID2 in the 300−400 nm (λ > 4200 M^{-1} cm^{-1}; Figure 1). The ID2/Iod system can also initiate the cationic polymerization of DVE-3 (see below the thiol−ene process).

2b. Free Radical Photopolymerization of Acrylates. The ID2/Iod or ID2/MDEA combinations slowly initiate the FRP of TMPTA in laminate using the low intensity halogen lamp (12 mW cm^{-2}) as shown in Figure 4, curve 1 and curve 4 for ID2/Iod (conversion = 8%) and ID2/MDEA (conversion = 23%), respectively. Under the higher intensity laser diode at 457 nm (100 mW cm^{-2}), the polymerization profiles are improved (Figure 4, curve 2 vs curve 1 for ID2/Iod; curve 5 vs curve 4 for ID2/MDEA). The ID2/Iod two-component system is better than CQ/Iod (conversion = 45% vs 35%) under the laser diode at 457 nm. The ID2/Iod/NVK and ID2/MDEA/R−Br (or R′−Cl) three-component systems are still more efficient (see Figure 4 and Table 2); the ID2/R′−Cl system can also work but to a lesser extent (conversion =16%; Figure 4, curve 7). Interestingly, R′−Cl is a better additive than R−Br (Figure 4, curve 9 vs curve 6) and an increase of [R′−Cl] improves the polymerization profile (Figure 4, curve 9 vs curve 8). In addition, the ID2/MDEA/R′−Cl combination (Figure 4, curve 8 and 9) exhibits a better efficiency than CQ/MDEA reference.

2c. Hybrid Cure: Photopolymerization of EPOX/TMPTA Blends. The ID2/Iod/NVK combination allows the formation of an interpenetrated polymer network (IPN) through a concomitant cationic/radical photopolymerization of an EPOX/TMPTA blend (50%/50% w/w) upon the household blue LED bulb exposure at 462 nm (Figure 5). Tack free coatings can be obtained after only 5 min. Although the final conversions (Table 3) of TMPTA (as observed in other systems[6,7,22]) are higher in laminate than under air, the observed high efficiency under air upon very low light intensity highlights the ability of the ID2 based systems to overcome the oxygen inhibition in a FRP process.

Table 2. TMPTA Conversions Obtained in Laminate upon Exposure to Different Visible Light Sources for 400 s in the Presence of ID2/Iod (0.5%/2%, w/w); ID2/Iod/NVK (0.5%/2%/3%, w/w/w); ID2/MDEA (0.5%/2%, w/w); ID2/MDEA/R−Br (0.5%/2%/3%, w/w/w); ID2/R′−Cl (0.5%/1%, w/w); ID2/MDEA/R′−Cl(1) (0.5%/2%/1%, w/w/w); ID2/MDEA/R′−Cl(3) (0.5%/2%/3%, w/w/w); CQ/Iod (0.5%/2%, w/w); or CQ/MDEA (0.5%/2%, w/w)

	% conversion	
	halogen lamp	laser diode (457 nm)
CQ/Iod	18	35
ID2/Iod	8	45
ID2/Iod/NVK	–	58
CQ/MDEA	35	46
ID2/MDEA	23	35
ID2/MDEA/R−Br	–	42
ID2/R′−Cl	–	16
ID2/MDEA/R′−Cl(1)	–	52
ID2/MDEA/R′−Cl(3)	–	60

2d. Thiol−Ene Photopolymerization. Thiol−ene photopolymerizations were mainly based on UV light. Remarkably, excellent conversion−time profiles are here obtained for the Trithiol/DVE-3 thiol−ene photopolymerization using the ID2/Iod combination under the household blue LED and the blue laser diode exposure (Figure 6). Even though the incident light intensity of the LED is 10 times lower than that of the laser diode, the polymerization profiles are quite similar (vinyl double bond conversions ∼98% in both cases). The S−H conversions (46% and 49%) are lower which probably reflects a concomitant CP polymerization of DVE-3. Remarkably, the polymerization of thick samples (from 1 mm to 5 mm) can also be achieved with the ID2/Iod system upon LED irradiation; this can be highly useful for applications requiring deep curing.

3. Photochemical Mechanisms of the Investigated Indanedione Derivatives. *3a. ID/Iod and ID/Iod/NVK Systems.* As demonstrated in other related PISs,[1,6−8] the expected reactions in the ID based systems (1−4) are likely the following:

$$ID \rightarrow {}^1ID\ (h\nu) \text{ and } {}^1ID \rightarrow {}^3ID \quad (1)$$

dx.doi.org/10.1021/ma402149g | Macromolecules 2014, 47, 26−34

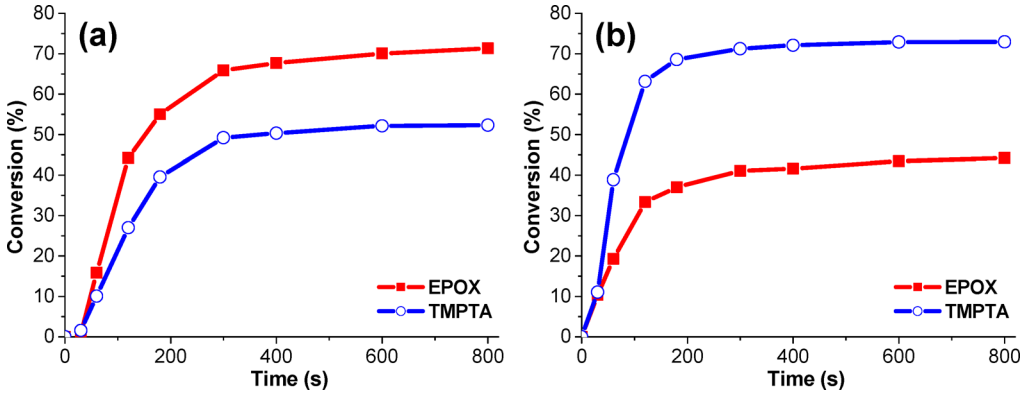

Figure 5. Photopolymerization profiles of an EPOX/TMPTA blend (50%/50%, w/w) in the presence of ID2/Iod/NVK (0.5%/2%/3%, w/w/w) under air (a) and in laminate (b) upon the blue LED bulb exposure at 462 nm.

Table 3. EPOX and TMPTA Final Conversions Obtained in the Polymerization of an EPOX/TMPTA Blend (50%/50%, w/w) under Air or in Laminate upon Exposure to the Household LED at 462 nm (t = 800 s) in the Presence of ID2/Iod/NVK (0.5%/2%/3%, w/w/w)

	EPOX conversion (%)	TMPTA conversion (%)
under air	71	52
in laminate	44	73

$$^{1,3}\mathrm{ID} + \mathrm{Ph_2I^+} \rightarrow \mathrm{ID^{\bullet +}} + \mathrm{Ph_2I^\bullet} \quad (2a)$$

$$\mathrm{ID^{\bullet +}} + \mathrm{Ph_2I^\bullet} \rightarrow \mathrm{ID^{\bullet +}} + \mathrm{Ph^\bullet} + \mathrm{Ph{-}I} \quad (2b)$$

$$\mathrm{Ph^\bullet} + \mathrm{NVK} \rightarrow \mathrm{Ph{-}NVK^\bullet} \quad (3a)$$

$$\mathrm{Ph{-}NVK^\bullet} + \mathrm{Ph_2I^+} \rightarrow \mathrm{Ph{-}NVK^+} + \mathrm{Ph^\bullet} + \mathrm{Ph{-}I} \quad (3b)$$

$$\mathrm{Ph^\bullet} + \mathrm{RS - H} \rightarrow \mathrm{Ph{-}H} + \mathrm{RS^\bullet} \quad (4a)$$

$$\mathrm{RS^\bullet} + \mathrm{R'{-}CH{=}CH_2} \rightarrow \mathrm{R'{-}CH^\bullet{-}CH_2SR} \quad (4b)$$

$$\mathrm{R'{-}CH^\bullet{-}CH_2SR} + \mathrm{RSH} \rightarrow \mathrm{R'{-}CH_2{-}CH_2SR} + \mathrm{RS^\bullet} \quad (4c)$$

In line with reaction 2, phenyl radicals are clearly observed in ESR spin trapping experiments on ID2/Iod (Figure 7).

The calculations of the free energy change ΔG for the corresponding electron transfer reaction 2a support a favorable singlet state process (ΔG = −1.71 eV using: oxidation potentials E_{ox} of the ID2 = 0.64 V, as measured by cyclic voltammetry—this work; reduction potential E_{red} = −0.2 V[1] for Iod; singlet state energy E_S =2.55 eV for ID2 as extracted from the UV−vis absorption and fluorescence emission spectra as usually done[25]). The results of the fluorescence quenching experiments were not reported due to the low fluorescence quantum yield of ID2 (~0.001). As in the previously studied indanedione derivatives,[8] no triplet state absorption is observed in laser flash photolysis experiments. However, a ^{3}ID2/Iod

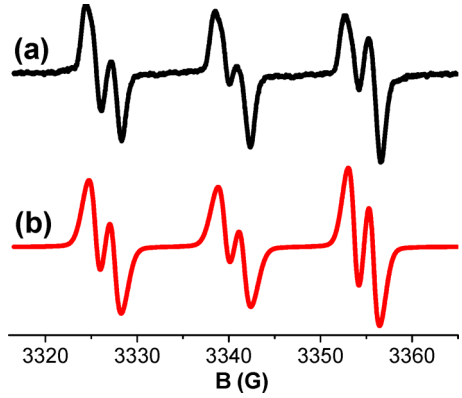

Figure 7. ESR spectra of the radicals generated in ID2/Iod and trapped by PBN in *tert*-butylbenzene: (a) experimental and (b) simulated spectra. PBN/phenyl radical adducts obtained in ID2/Iod: a_N = 14.1 G; a_H = 2.1 G; reference values.[23,24]

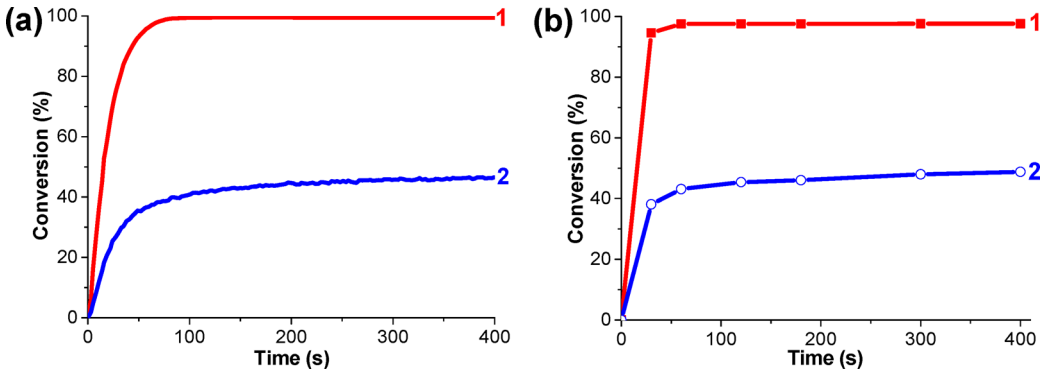

Figure 6. Photopolymerization profiles of Trithiol/DVE-3 blend (40%/60%, n/n; 57%/43%, w/w) in laminate in the presence of ID2/Iod (0.5%/2%, w/w) upon the (a) blue laser diode at 457 nm and (b) blue LED bulb at 462 nm exposure. Curve 1: DVE-3 (vinyl double bond) conversion. Curve 2: trithiol (S−H) conversion.

dx.doi.org/10.1021/ma402149g | *Macromolecules* 2014, 47, 26−34

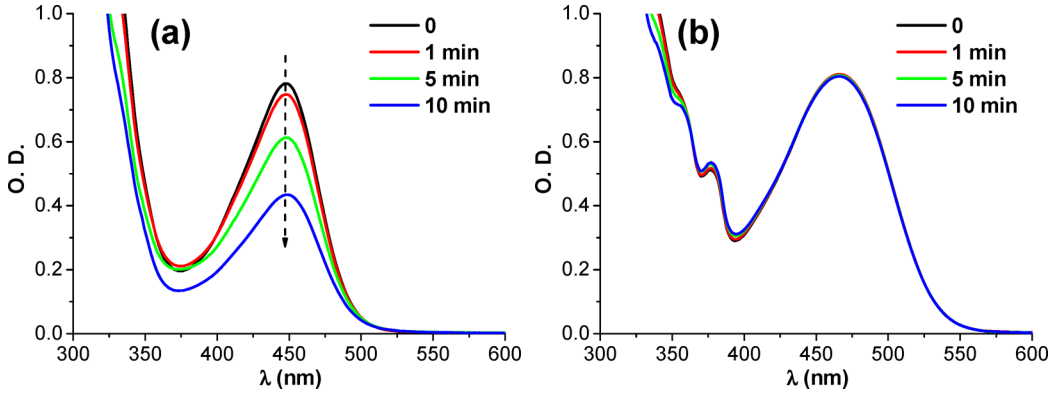

Figure 8. Steady state photolysis of (a) ID2/Iod and (b) ID3/Iod in acetonitrile upon the halogen lamp exposure. [Iod] = 45 mM. UV−vis spectra recorded at different irradiation times.

electron transfer in the triplet state should be feasible as ΔG is negative (−1.34 eV; the triplet state energy level is 2.18 eV as calculated at UB3LYP/6-31G* level). Contrary to ID2, no fluorescence is detected in ID1, ID3 and ID4.

The steady state photolysis of ID2/Iod and ID3/Iod in acetonitrile (Figure 8; halogen lamp exposure; under air) confirms a noticeable reactivity difference (very fast bleaching of ID2/Iod and tiny bleaching of ID3/Iod) which is responsible for the relative polymerization abilities. Similarly, the very little bleaching of ID1/Iod and the increase of the light absorption at 386 nm in ID4/Iod (Figure S1 in the Supporting Information) are also consistent with their poor efficiency.

3b. ID/Amine/Alkyl Halide System. ID2/MDEA, ID2/MDEA/R−Br, and ID2/MDEA/R′−Cl systems can work according to reactions 5−9 as already proposed in other dye systems.[13,26−28] Reactions 5 and 6 are probably in competition as their free energy changes ΔG for the corresponding electron transfer reaction are favorable: −1.13 eV for ^{1}ID2/R−Br; −0.76 eV for ^{3}ID2/R−Br; −0.73 eV for ^{1}ID2/MDEA; −0.36 eV for ^{3}ID2/MDEA. As the reduction potentials of R−Br[29] and R′−Cl[30] are similar (−0.78 V), reactions 6−8 probably occur for R−Br and R′−Cl. The higher efficiency of ID2/MDEA/R′−Cl compared to ID2/MDEA/R−Br in FRP probably results from a better reactivity of the generated radicals (R′$^\bullet$ vs R$^\bullet$) toward the initiation of the polymerization reaction.

$$^{1,3}\text{ID2} + \text{MDEA} \rightarrow \text{ID2}^{\bullet -} + \text{MDEA}^{\bullet +} \rightarrow \text{ID2} - \text{H}^\bullet + \text{MDEA}_{(-\text{H})}{}^\bullet \quad (5)$$

$$^{1,3}\text{ID2} + \text{R}'-\text{Cl (or R}-\text{Br}) \rightarrow \text{ID2}^{\bullet +} + (\text{R}'-\text{Cl})^{\bullet -}\ [\text{or } (\text{R}-\text{Br})^{\bullet -}] \quad (6)$$

$$\text{ID2}^{\bullet -} + \text{R}'-\text{Cl (or R}-\text{Br}) \rightarrow \text{ID2} + (\text{R}'-\text{Cl})^{\bullet -}\ [\text{or } (\text{R}-\text{Br})^{\bullet -}] \quad (7)$$

$$\text{ID2}-\text{H}^\bullet + \text{R}'-\text{Cl (or R}-\text{Br}) \rightarrow \text{ID2} + \text{H}^+ + (\text{R}'-\text{Cl})^{\bullet -}\ [\text{or } (\text{R}-\text{Br})^{\bullet -}] \quad (8)$$

$$(\text{R}'-\text{Cl})^{\bullet -}\ [\text{or } (\text{R}-\text{Br})^{\bullet -}] \rightarrow \text{R}'^\bullet + \text{Cl}^-\ [\text{or R}^\bullet + \text{Br}^-] \quad (9)$$

3c. Initiation Mechanisms. On the basis of the above investigations, the higher polymerization efficiency of ID2/Iod compared to that of ID1 (or ID3, ID4)/Iod may be associated with (i) the better light absorption properties of ID2, (ii) the higher yield in reactive species (Ph$^\bullet$ and ID$^{\bullet +}$; reaction 2) and (iii) the higher reactivity of the radical cation (ID2$^{\bullet +}$) in CP and FRPCP processes. In ID2 based PISs, the initiating species are: ID2$^{\bullet +}$ and Ph-NVK$^+$ (reactions 1−3)[21] for the CP/FRPCP of EPOX; the Ph$^\bullet$, Ph-NVK$^\bullet$, aminoalkyl (MDEA $_{(-H)}{}^\bullet$) and R′$^\bullet$ (or R$^\bullet$) radicals for the FRP of TMPTA (reactions 1−3, 5-9); the thiyl radicals (reactions 1−2, 4) for the thiol−ene photopolymerization.

3d. ID2/Iod/NVK System: A Photoinitiating System for the Ag(0) Nanoparticles Formation. Interestingly, upon a low intensity household blue LED exposure, the ID2/Iod/NVK system in the presence of a silver salt ($AgSbF_6$) is also able to generate Ag(0) nanoparticles NP (Figure 9). Remarkably, the

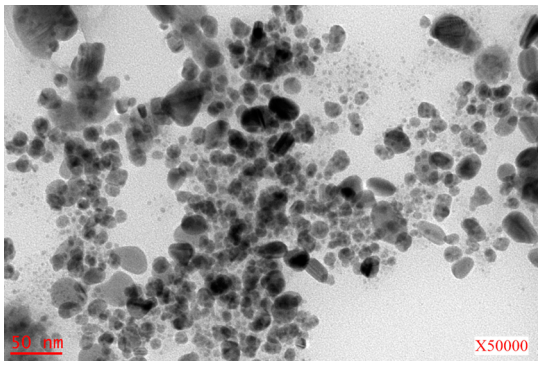

Figure 9. Observed TEM micrograph for the irradiation of a ID2/Iod/NVK/$AgSbF_6$ solution in acetonitrile (blue LED bulb at 462 nm; exposure 10 min).

ID2/Iod/NVK/$AgSbF_6$ system is able to both initiate the polymerization reactions (see above) and generate the Ag(0) NPs, i.e., the synthesized Ag(0) NPs are in situ embedded in the synthesized polymers. As shown recently,[31] the reduction of the silver salt (10) can be associated with the easy oxidation of Ph-NVK$^\bullet$ (generated in 3a) as no Ag(0) NP formation is observed when using the ID2/Iod/$AgSbF_6$ system.

$$\text{Ph}-\text{NVK}^\bullet + \text{Ag}^+ \rightarrow \text{Ph}-\text{NVK}^+ + \text{Ag}(0) \quad (10)$$

CONCLUSION

The newly developed indanedione derivative ID2 in combination with an iodonium salt Iod and optionally *N*-vinylcarbazole NVK can be used as a high performance visible light or blue light sensitive PIS to efficiently initiate the cationic polymer-

dx.doi.org/10.1021/ma402149g | *Macromolecules* 2014, 47, 26−34

ization of EPOX, the radical polymerization of TMPTA, the TMPTA/EPOX blend IPN polymerization, and the thiol−ene polymerization as well under low light intensities. In addition, the ID2/amine/phenacyl bromide or the ID2/amine/2,4,6-tris(trichloromethyl)-1,3,5-triazine combinations are also efficient for the radical polymerization of TMPTA. Moreover, ID2 is more efficient than the well-known visible light sensitizer CQ and can be useful to overcome the oxygen inhibition. The proposed structure is also very efficient for the in situ formation of Ag(0) nanoparticles. This present research confirms that the design of push−pull photoinitiators is a promising way to develop highly absorbing compounds in the blue wavelength range which ensures polymerization reactions under low intensity light sources.

■ ASSOCIATED CONTENT

Supporting Information

Figure S1, steady state photolysis of ID1/Iod and ID4/Iod in acetonitrile. This material is available free of charge via the Internet at http://pubs.acs.org/.

■ AUTHOR INFORMATION

Corresponding Authors

* E-mail: jacques.lalevee@uha.fr (J.L.).
* E-mail: didier.gigmes@univ-amu.fr (D.G.).

Present Address

[⊥]Formerly at: ENSCMu-UHA, 3 rue Alfred Werner, 68093 Mulhouse Cedex, France.

Notes

The authors declare no competing financial interest.

■ ACKNOWLEDGMENTS

J.L. thanks the Institut Universitaire de France for the financial support.

■ REFERENCES

(1) Fouassier, J. P.; Lalevée, J. *Photoinitiators for Polymer Synthesis-Scope, Reactivity, and Efficiency*; Wiley-VCH Verlag GmbH & Co. KGaA: Weinheim, Germany, 2012.

(2) Crivello, J. V. *Photoinitiators for Free Radical, Cationic and Anionic Photopolymerization*, 2nd ed.; John Wiley & Sons: Chichester, U.K., 1998.

(3) Fouassier, J. P.; Lalevée, J. *RSC Adv.* **2012**, *2*, 2621−2629.

(4) Fouassier, J. P.; Morlet-Savary, F.; Lalevée, J.; Allonas, X.; Ley, C. *Materials* **2010**, *3*, 5130−5142.

(5) (a) Crivello, J. V.; Aldersley, M. F. *J. Polym. Sci., Part A: Polym. Chem.* **2013**, *51*, 801−814. (b) Sangermano, M.; Sordo, F.; Chiolerio, A.; Yagci, Y. *Polymer* **2013**, *54*, 2077−2080. (c) Fabbri, P.; Valentini, L.; Bittolo Bon, S.; Foix, D.; Pasquali, L.; Montecchi, M.; Sangermano, M. *Polymer* **2012**, *53*, 6039−6044. (d) Yang, J.; Tang, R.; Shi, S.; Nie, J. *Photochem. Photobiol. Sci.* **2013**, *12*, 923−929. (e) Gong, T.; Adzima, B. J.; Baker, N. H.; Bowman, C. N. *Adv. Mater.* **2013**, *25*, 2024−2028. (f) Kitano, H.; Ramachandran, K.; Bowden, N. B.; Scranton, A. B. *J. Appl. Polym. Sci.* **2013**, *128*, 611−618. (g) Bai, J.; Shi, Z. *J. Appl. Polym. Sci.* **2013**, *128*, 1785−1791. (h) Esen, D. S.; Arsu, N.; Da Silva, J. P.; Jockusch, S.; Turro, N. J. *J. Polym. Sci., Part A: Polym. Chem.* **2013**, *51*, 1865−1871. (i) Shih, H.; Lin, C.-C. *Macromol. Rapid Commun.* **2013**, *34*, 269−273. (j) Balta, D. K.; Arsu, N. *J. Photochem. Photobiol. A: Chem.* **2013**, *257*, 54−59. (k) Doğruyol, S. K.; Doğruyol, Z.; Arsu, N. *J. Lumin.* **2013**, *138*, 98−104. (l) Tar, H.; Esen, D. S.; Aydin, M.; Ley, C.; Arsu, N.; Allonas, X. *Macromolecules* **2013**, *46*, 3266−3272. (m) Korkut, S. E.; Temel, G.; Balta, D. K.; Arsu, N.; Şener, M.K. J. *Lumin.* **2013**, *136*, 389−394. (n) Santos, W. G.; Schmitt, C. C.; Neumann, M. G. *J. Photochem. Photobiol. A: Chem.* **2013**, *252*, 124−130. (o) Corakci, B.; Hacioglu, S. O.; Toppare, L.; Bulut, U. *Polymer* **2013**, *54*, 3182−3187. (p) Podsiadły, R.; Strzelczyk, R. *Dyes Pigm.* **2013**, *97*, 462−468. (q) Shen, K.; Li, Y.; Liu, G.; Li, Y.; Zhang, X. *Prog. Org. Coat.* **2013**, *76*, 125−130. (r) Xiao, Q.; Ji, Y.; Xiao, Z.; Zhang, Y.; Lin, H.; Wang, Q. *Chem. Commun.* **2013**, *49*, 1527−1529.

(6) (a) Xiao, P.; Dumur, F.; Tehfe, M.-A.; Graff, B.; Gigmes, D.; Fouassier, J. P.; Lalevée, J. *Macromol. Chem. Phys.* **2013**, DOI: 10.1002/macp.201300363. (b) Xiao, P.; Dumur, F.; Tehfe, M. A.; Graff, B.; Gigmes, D.; Fouassier, J. P.; Lalevée, J. *Polymer* **2013**, *54*, 3458−3466.

(7) Xiao, P.; Dumur, F.; Frigoli, M.; Tehfe, M.-A.; Morlet-Savary, F.; Graff, B.; Fouassier, J. P.; Gigmes, D.; Lalevée, J. *Polym. Chem.* **2013**, *4*, 5440−5448.

(8) Tehfe, M. A.; Dumur, F.; Graff, B.; Gigmes, D.; Fouassier, J. P.; Lalevée, J. *Macromolecules* **2013**, *46*, 3332−3341.

(9) Dumur, F.; Contal, E.; Wantz, G.; Phan, T. N. T.; Bertin, D.; Gigmes, D. *Chem.—Eur. J.* **2013**, *19*, 1373−1384.

(10) Tehfe, M. A.; Dumur, F.; Contal, E.; Graff, B.; Gigmes, D.; Fouassier, J. P.; Lalevée, J. *Macromol. Chem. Phys.* **2013**, *214*, 2189−2201.

(11) Tehfe, M. A.; Dumur, F.; Graff, B.; Morlet-Savary, F.; Gigmes, D.; Fouassier, J. P.; Lalevee, J. *Polym. Chem.* **2013**, *4*, 3866−3875.

(12) Tehfe, M. A.; Lalevée, J.; Telitel, S.; Sun, J.; Zhao, J.; Graff, B.; Morlet-Savary, F.; Fouassier, J. P. *Polymer* **2012**, *53*, 2803−2808.

(13) Tehfe, M. A.; Lalevée, J.; Morlet-Savary, F.; Graff, B.; Blanchard, N.; Fouassier, J. P. *Macromolecules* **2012**, *45*, 1746−1752.

(14) Xiao, P.; Lalevée, J.; Allonas, X.; Fouassier, J. P.; Ley, C.; El Roz, M.; Shi, S. Q.; Nie, J. *J. Polym. Sci., Part A: Polym. Chem.* **2010**, *48*, 5758−5766.

(15) Fouassier, J. P. *Photoinitiator, Photopolymerization and Photocuring: Fundamentals and Applications*; Hanser Publishers: Munich Vienna, and New York, 1995.

(16) Rehm, D.; Weller, A. *Isr. J. Chem.* **1970**, *8*, 259−271.

(17) Foresman, J. B.; Frisch, A. *Exploring Chemistry with Electronic Structure Methods*; Gaussian. Inc.: Pittsburgh, PA, 1996.

(18) Frisch, M. J.; Trucks, G. W.; Schlegel, H. B.; Scuseria, G. E.; Robb, M. A.; Cheeseman, J. R.; Zakrzewski, V. G.; Montgomery, J. A.; Stratmann, J. R. E.; Burant, J. C.; Dapprich, S.; Millam, J. M.; Daniels, A. D.; Kudin, K. N.; Strain, M. C.; Farkas, O.; Tomasi, J.; Barone, V.; Cossi, M.; Cammi, R.; Mennucci, B.; Pomelli, C.; Adamo, C.; Clifford, S.; Ochterski, J.; Petersson, G. A.; Ayala, P. Y.; Cui, Q.; Morokuma, K.; Salvador, P.; Dannenberg, J. J.; Malick, D. K.; Rabuck, A. D.; Raghavachari, K.; Foresman, J. B.; Cioslowski, J.; Ortiz, J. V.; Baboul, A. G.; Stefanov, B. B.; Liu, G.; Liashenko, A.; Piskorz, P.; Komaromi, I.; Gomperts, R.; Martin, R. L.; Fox, D. J.; Keith, T.; Al-Laham, M. A.; Peng, C. Y.; Nanayakkara, A.; Challacombe, M.; Gill, P. M. W.; Johnson, B.; Chen, W.; Wong, M. W.; Andres, J. L.; Gonzalez, C.; Head-Gordon, M.; Replogle, E. S.; Pople, J. A. *Gaussian 03, Revision B-2*; Gaussian, Inc.: Pittsburgh PA, 2003.

(19) Lalevée, J.; Blanchard, N.; Tehfe, M. A.; Peter, M.; Morlet-Savary, F.; Gigmes, D.; Fouassier, J. P. *Polym. Chem.* **2011**, *2*, 1986−1991.

(20) Tehfe, M. A.; Lalevée, J.; Morlet-Savary, F.; Blanchard, N.; Fries, C.; Graff, B.; Allonas, X.; Louerat, F.; Fouassier, J. P. *Eur. Polym. J.* **2010**, *46*, 2138−2144.

(21) Lalevée, J.; Tehfe, M. A.; Zein-Fakih, A.; Ball, B.; Telitel, S.; Morlet-Savary, F.; Graff, B.; Fouassier, J. P. *ACS Macro Lett.* **2012**, *1*, 802−806.

(22) Xiao, P.; Simonnet-Jégat, C.; Dumur, F.; Schrodj, G.; Tehfe, M. A.; Fouassier, J. P.; Gigmes, D.; Lalevée, J. *Polym. Chem.* **2013**, *4*, 4526−4530.

(23) Tehfe, M. A.; Lalevée, J.; Telitel, S.; Contal, E.; Dumur, F.; Gigmes, D.; Bertin, D.; Nechab, M.; Graff, B.; Morlet-Savary, F.; Fouassier, J. P. *Macromolecules* **2012**, *45*, 4454−4460.

(24) Lalevée, J.; Blanchard, N.; Tehfe, M. A.; Morlet-Savary, F.; Fouassier, J. P. *Macromolecules* **2010**, *43*, 10191−10195.

(25) Tehfe, M. A.; Lalevée, J.; Morlet-Savary, F.; Graff, B.; Blanchard, N.; Fouassier, J. P. *ACS Macro Lett.* **2012**, *1*, 198−203.

(26) Tehfe, M. A.; Dumur, F.; Graff, B.; Morlet-Savary, F.; Fouassier, J.-P.; Gigmes, D.; Lalevée, J. *Macromolecules* **2013**, *46*, 3761−3770.

(27) (a) Grotzinger, C.; Burget, D.; Jacques, P.; Fouassier, J. P. *Macromol. Chem. Phys.* **2001**, *202*, 3513−3522. (b) Fouassier, J. P.; Allonas, X.; Burget, D. *Prog. Org. Coat.* **2003**, *47*, 16−36.
(28) Kabatc, J.; Zasada, M.; Pączkowski, J. *J. Polym. Sci., Part A: Polym. Chem.* **2007**, *45*, 3626−3636.
(29) Renaud, J.; Scaiano, J. C. *Can. J. Chem.* **1996**, *74*, 1724−1730.
(30) Wallraff, G.; Baier, M.; Diaz, A.; Miller, R. *J. Inorg. Organomet. Polym.* **1992**, *2*, 87−102.
(31) Mokbel, H.; Dumur, F.; Telitel, S.; Vidal, L.; Xiao, P.; Versace, D.-L.; Tehfe, M. A.; Morlet-Savary, F.; Graff, B.; Fouassier, J. P.; Gigmes, D.; Toufaily, J.; Hamieh, T.; Lalevee, J. *Polym. Chem.* **2013**, DOI: 10.1039/c3py00846k.